Circadian gating of the cell cycle revealed in single cyanobacterial cells

Qiong Yang[1,*], **Bernardo F. Pando**[1,*], **Guogang Dong**[3], **Susan S. Golden**[3], and **Alexander van Oudenaarden**[1,2,†]

[1]Department of Physics, Massachusetts Institute of Technology, Cambridge MA 02139, USA.

[2]Department of Biology, Massachusetts Institute of Technology, Cambridge MA 02139, USA.

[3]Center for Chronobiology and Division of Biological Sciences, University of California-San Diego, La Jolla, CA 92093, USA.

Abstract

Although major progress has been made in uncovering the machinery underlying individual biological clocks, much less is known about how multiple clocks coordinate their oscillations. We present a general framework that describes coupled cyclic processes in single cells and apply this to the interaction between the circadian and cell-division cycles in the cyanobacterium *Synechococcus elongatus*. We simultaneously track cell-division events and circadian phases of individual cells and use this information to determine when cell-cycle progression is slowed down as a function of circadian and cell-cycle phases. We infer that cell-cycle progression in cyanobacteria slows down during a specific circadian interval, but is uniform across cell-cycle phase. Our framework is applicable to the quantification of the coupling between any biological oscillators in other organisms.

Cyclic processes in biology span a wide dynamic range from the sub-second periods of neural spike trains to annual rhythms in animal and plant reproduction (1–3). Even an individual cell exposed to a constant environment may exhibit many parallel periodic activities with different frequencies such as glycolytic, cell cycle, and circadian oscillations (4–8). Therefore it is important to elucidate how different oscillators couple to each other (9). In several unicellular organisms and higher vertebrates it has been shown that the circadian system affects whether cell division is permitted (10–15); similarly, the yeast metabolic cycle restricts when the cell divides (16). In this work we integrate theoretical and experimental approaches to investigate how the circadian and cell-division subsystems are coupled together in single cells of the cyanobacterium *Synechococcus elongatus*.

In order to quantify how one clock couples to the other, we built a model by describing the state of each cell with its circadian and cell cycle phases, $\theta(t)$ and $\phi(t)$, both periodic from 0 to 2π (17–18). Given the robustness of circadian oscillations to environmental and intracellular variations, it is believed that the circadian system progresses independently of cell cycle (19–20). Hence, we propose that the progression rate of the circadian phase is constant except for some noise whereas the speed of cell-cycle progression could depend on both the circadian and cell-cycle phases. We describe the time evolution of the phases of these clocks by two Langevin equations

†To whom correspondence should be addressed: avano@mit.edu.
*These authors contributed equally

$$\begin{cases} \frac{d\theta}{dt} = v_0 + \xi_\theta \\ \frac{d\phi}{dt} = v\gamma(\phi, \theta) + \xi_\phi \end{cases}$$

where ξ_ϕ and ξ_ϕ are white-noise terms representative of intrinsic fluctuations, v_0 is the speed of the circadian clock, v roughly describes the average speed of cell cycle progression and $\gamma(\phi, \theta)$, the coupling, is a non-negative function describing how the state of the clocks affects cell-cycle speed. Regions in (ϕ, θ) space where γ is close to zero indicate slowing down of cell cycle progression and are usually referred to as "gates" [11].

This model can be simulated using Monte Carlo methods or solved using Fokker-Planck techniques [21], to explore whether the cell-cycle gets synchronized to circadian signals and how the timing of cell divisions is distributed throughout the day. A division event happens as the variable ϕ crosses the 2π boundary [22]. Without gating ($\gamma = 1$), the two clocks are uncorrelated and cells divide uniformly throughout the day (Fig. 1, left column). However, in the presence of a gate, cell-cycle states synchronize to the circadian signal (Fig. 1, middle column), similarly to how nonlinear oscillators lock into periodic forcings [23–24]. For cell-cycle speeds comparable to that of the circadian clock, cells tend to divide at a single circadian phase; however, as v is increased, the number of times in the day at which divisions are likely to take place also increases, leading to multimodal distributions of division phases (Fig. 1, right column, Fig. S2) [25]. This feature is generic and independent of the specific shape of the coupling function used [17–18, 23] (Fig. S8).

To quantify this gating phenomenon experimentally, we investigated the interaction between the circadian and cell cycle clocks in the cyanobacterium *S. elongatus* PCC 7942. A previous study at the population level indicated the existence of circadian gating in this organism [11]. To explicitly explore how one clock gates the other, we took a single-cell fluorescence microscopy approach and simultaneously tracked both clocks' dynamics in individual cyanobacteria as they proliferated under a constant light environment (Fig. 2A). Circadian dynamics in each cell are faithfully reported by the SsrA-tagged yellow fluorescent protein (YFP-SsrA) under the rhythmic *kaiBC* promoter [26]. This promoter drives the endogenous expression of the *kaiB* and *kaiC* genes which, together with *kaiA*, form the central protein circuit that orchestrates circadian rhythms in cyanobacteria. We defined the circadian phase as the time from the nearest previous *YFP* peak normalized by the circadian period (Fig. 2B); our proxy for cell-cycle phase progression involved tracking individual cells' growth over time [21]. We detected nearly all cell divisions, recorded the corresponding circadian phases θ_d, and measured each cell's cell-cycle duration τ (Fig. 2C).

We first performed an experiment under a light intensity of about $25\ \mu E\ m^{-2}\ s^{-1}$ (Fig. 3, left column), which gave an average cell-cycle speed comparable to that of the circadian clock: $\tau = (18 \pm 7)$ h (mean $\pm$ s.d.). To test whether cell-cycle phases were indeed synchronized by circadian signals, we collected all single-cell traces, aligned them based on their circadian phases [21], and constructed histograms of the circadian phases at division (Fig. 3). Rather than the distribution expected for uncorrelated clocks [21], we found a singly-peaked distribution of divisions per circadian cycle, indicating that divisions happened mostly at an specific circadian time.

In theory, we expect a similar locking if we double the relative speed of the cell cycle to that of the circadian clock, with divisions taking place now at two specific circadian phases. Although the period of the circadian clock is nearly constant over a range of growth conditions, cell-cycle progression is sensitive to environmental light intensity. These properties allowed us to tune the cell-cycle speed while keeping a constant circadian rate.

With a light intensity of about 50 µE m^{-2} s^{-1} the average cell-cycle duration shortened to (10 ± 4) h (mean $\pm$ s.d), whereas the average circadian period stayed around 24 h. Hence, we obtained about a two-fold increase in the relative speed of the two oscillators. We observed two peaks of cell divisions per circadian cycle (Fig. 3), in agreement with our theoretical analysis (Fig. 1).

A better understanding of the gating phenomenon relies on a direct measurement of the correlation between the two clocks for each single cell. We summarized such interaction in scatter plots of the circadian phase at cell division, θ_d, and the cell-cycle duration of the corresponding cell τ (Fig. 4A). We fit our model to both datasets simultaneously, considering the same coupling function $\gamma(\phi, \theta)$ and noise strengths for the two experiments. We allowed only the parameter ν to vary across the two experimental conditions and included only coupling functions representative of a single maximal gate (21). This procedure yielded reasonable fits for both data sets (Fig. 4B), indicating that it is possible to explain the interaction between the clocks in the two different conditions using the same coupling function.

The inferred coupling function is shown in Fig. 4C. To relate the phase θ to the real circadian phase, we considered that the *YFP* protein has a non-negligible lifetime, which makes the reported signal lag behind the day-night cycle. Measurements on cell cultures that had been synchronized by three 12:12 light-dark cycles indicate that the signal peak (identified as $\theta = 0$) lags (19 h $\pm$ 1 h) behind the day start (21), in agreement with previous studies (26). Considering this delay, the inferred coupling function shows a gate positioned at 17 h after the day start, lasting for (6.1 ± 0.3) h (Fig. 4D) and distributed essentially uniformly across cell cycle stages (Fig. 4E). We conclude that in this case the circadian signal acts on the cell cycle by repressing essentially all its stages in the middle subjective night.

This suggests that in *Synechococcus* regulation of cell cycle progression by the circadian system may be more extensive than interactions between circadian signals and proteins associated with specific cell cycle processes. The molecular mechanism coupling the two oscillators in *Synechococcus* might be fundamentally different than that found in mammalian cells in which the expression of several key cell cycle regulators, including Wee1 and Cdc2, was found to be regulated by the circadian oscillator (12). Recent data start to reveal molecular interactions responsible for coupling the cell-cycle and circadian oscillator in cyanobacteria (27). Our results suggest that it is unlikely that gating is exclusively regulated by just one mechanism that imposes a checkpoint at a specific cell-cycle stage. Instead, it might involve a more overarching regulation scheme, perhaps analogous to how circadian clocks coordinate genomewide gene expression at specific circadian times (28).

The gating phenomenon seems to be universally conserved from some prokaryotes to mammals. It would be interesting to understand why gating is important to cells. In cyanobacteria, cells enhance their fitness when their circadian period resonates with external light-dark cycles (29) and perhaps a similar resonance between circadian and cell-cycle clocks might lead to a fitness increase. Consistent with this, our results suggest that cell growth is prohibited during the middle of the night when energy is most limited.

The proposed theoretical approach is generally applicable to any set of coupled cyclic processes in which some information about the phases of each clock could be independently measured and will lead to a deeper understanding of how multiple periodic processes coordinate to control the dynamic state of the cell.

Supplementary Material

Refer to Web version on PubMed Central for supplementary material.

References and Notes

1. Goldbeter, A. Biochemical oscillations and cellular rhythms: the molecular bases of periodic and chaotic behaviour. Cambridge, UK: Cambridge University Press; 1996.

2. Glass, L.; Mackey, MC. From clocks to chaos: the rhythms of life. Princeton, NJ: Princeton University Press; 1988.

3. Maroto, M.; Monk, NAM. Cellular oscillatory mechanisms. New York, NY: Springer Science +Business Media; 2008.

4. Dyachok O, Isakov Y, Sagetorp J, Tengholm A. Nature. 2006; 439:349. [PubMed: 16421574]

5. Kholodenko BN. Nat. Rev. Mol. Cell Biol. 2006; 7:165. [PubMed: 16482094]

6. Panda S, Hogenesch JB, Kay SA. Nature. 2002; 417:329. [PubMed: 12015613]

7. Goldbeter A. Curr. Biol. 2008; 18:R751. [PubMed: 18786378]

8. Ishiura M, et al. Science. 1998; 281:1519. [PubMed: 9727980]

9. Méndez-Ferrer S, Lucas D, Battista M, Frenette PS. Nature. 2008; 452:442. [PubMed: 18256599]

10. Nagoshi E, et al. Cell. 2004; 119:693. [PubMed: 15550250]

11. Mori T, Binder B, Johnson CH. Proc. Natl. Acad. Sci. U.S.A. 1996; 93:10183. [PubMed: 8816773]

12. Matsuo T, et al. Science. 2003; 302:255. [PubMed: 12934012]

13. Dekens MPS, et al. Curr. Biol. 2003; 13:2051. [PubMed: 14653994]

14. Hirayama J, Cardone L, Doi M, Sassone-Corsi P. Proc. Natl. Acad. Sci. U.S.A. 2005; 102:10194. [PubMed: 16000406]

15. Salter MG, Franklin KA, Whitelam GC. Nature. 2003; 426:680. [PubMed: 14668869]

16. Tu BP, Kudlicki A, Rowicka M, McKnight SL. Science. 2005; 310:1152. [PubMed: 16254148]

17. Winfree, AT. The geometry of biological time. Rensselaer, NY: Springer-Verlag; 1980.

18. Strogatz, HS. Nonlinear dynamics and chaos. Cambridge, MA: Perseus Books Publishing; 1994.

19. Mori T, Johnson CH. J Bacteriol. 2001 Apr.183:2439. [PubMed: 11274102]

20. Mihalcescu I, Hsing W, Leibler S. Nature. 2004; 430:81. [PubMed: 15229601]

21. Details are available in the supporting materials on *Science Online*.

22. This identification is valid independently of the relationship between phases inside this range and specific biological processes.

23. Glass L. Nature. 2001; 410:277. [PubMed: 11258383]

24. Charvin G, Cross FR, Siggia ED. Proc. Natl. Acad. Sci. U.S.A. 2009; 106:6632. [PubMed: 19346485]

25. Zámborszky J, Hong CI, Csikász Nagy A. J Biol Rhythms. 2007; 22:542. [PubMed: 18057329]

26. Chabot JR, Pedraza JM, Luitel P, Oudenaarden Av. Nature. 2007; 450:1249. [PubMed: 18097413]

27. Dong G, et al. Cell. 2010

28. Imai K, Nishiwaki T, Kondo T, Iwasaki H. J. Biol. Chem. 2004; 279:36534. [PubMed: 15229218]

29. Ouyang Y, Andersson CR, Kondo T, Golden SS, Johnson CH. Proc Natl Acad Sci U S A. 1998; 95:8660. [PubMed: 9671734]

30. The authors would like to thank J. Gore, P. Luitel, C. Engert and S. Klemm for helpful discussions and/or experimental help. This work was supported by NSF grant PHY-0548484, NIH grant R01-GM068957, and R01-GM062419.
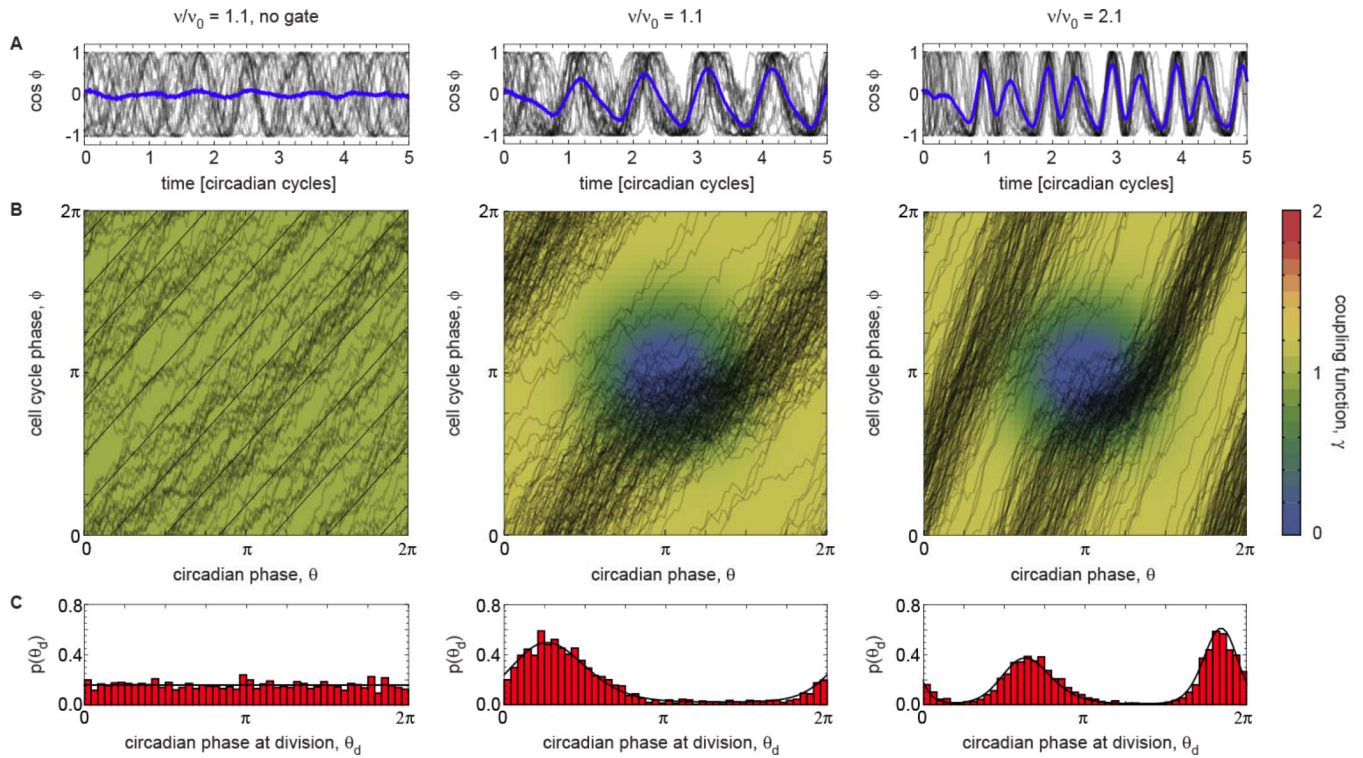
Fig. 1. Synchronization of cell cycle phases to circadian signals

Monte Carlo simulations of the evolution of a population of cells with an initially uniform distribution of cell cycle phases and synchronous circadian signals. (**A**) Cosine projection of cell cycle phases of 10 traces and average across 100 traces. The ratio of the average speed of cell cycle progression and circadian speed v/v_0 is 1.1 for the left and middle columns and 2.1 for the right column. The left column represents a situation in which there is no gating ($\gamma = 1$) whereas in the other columns the shape of the coupling function is color coded. (**B**) Color-coded coupling function and steady state organization of trajectories in (ϕ, θ) space. In the no-gate case, straight lines show the deterministic behavior. (**C**) Steady-state probability distribution of circadian phases at which divisions take place, $p(\theta_d)$; the bars are the results of Monte-Carlo simulations whereas the solid line represents the result of a Fokker-Planck computation (21). Parameters used: $= D_\theta = 0$, $D_\phi = 0.1v_0$, and, for the last two columns, $\alpha = \beta = 4$, $\theta_0 = \phi_0 = \pi$, where D_θ and D_ϕ correspond to the noise strengths of the circadian and cell-cycle oscillators, α, β, θ_0, and ϕ_0 are parameters defining the shape and position of the coupling function (21).
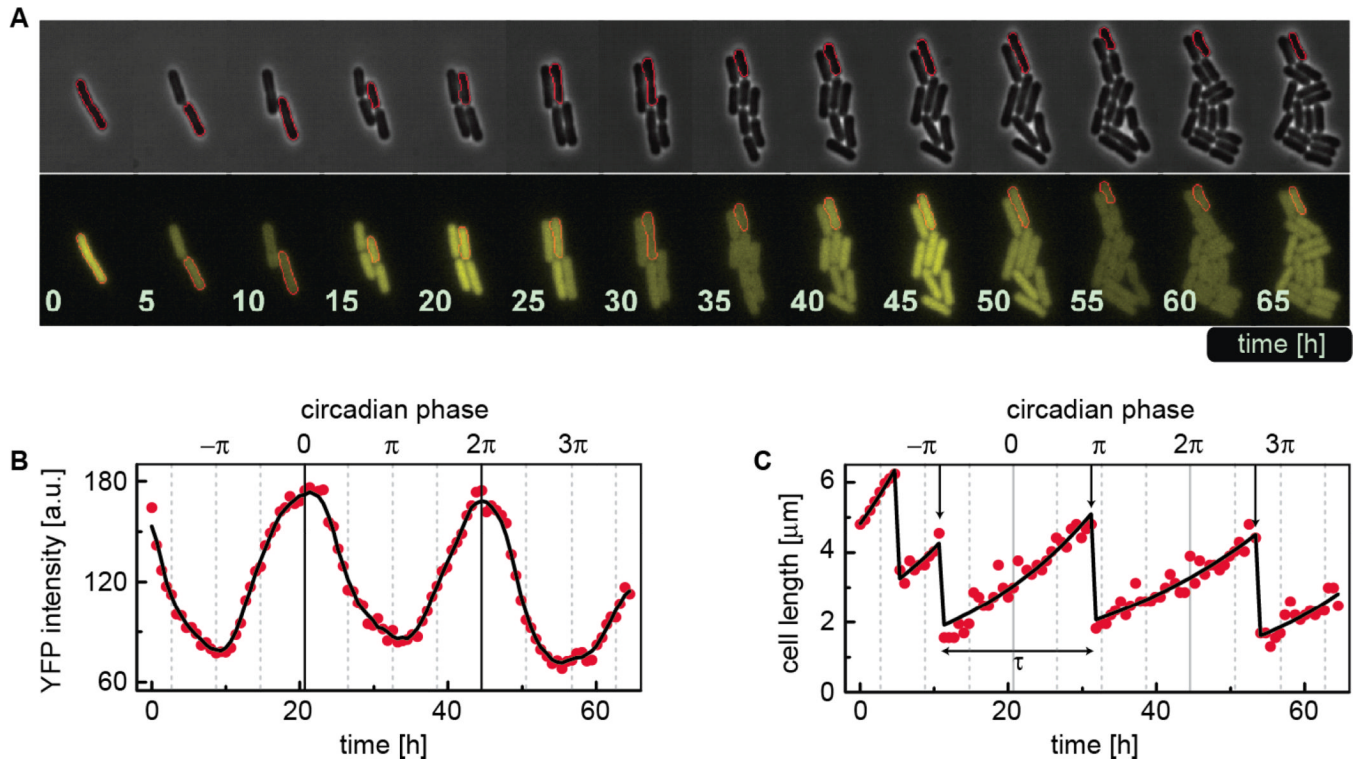
Fig. 2. Timelapse microscopy allows single cell measurements of circadian and cell cycle states
(**A**) Phase contrast (upper panel) and *YFP* images (lower panel) of a colony tracked over a few days. (**B**) *YFP* trace for the cell outlined in red in **A** (red dots: *YFP* intensity; black line: 10-point running average). (**C**) Length dynamics of the same cell; dots: instantaneous cell length; black line: exponential fit; vertical arrows: circadian phases at cell divisions; the horizontal double arrow illustrates the cell cycle lifespan τ for one cell.
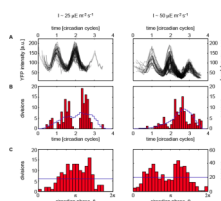
Fig. 3. Circadian gating as observed in single cells
(**A**) *YFP* traces for cells in 18 colonies shifted so as to maximize overlap. (**B**) Histogram of the timing of division events. Blue trace: expectation for uncorrelated clocks. (**C**) Histogram of the timing of division events across the circadian cycle (plot constructed as in **B** but measuring time relative to the start of each circadian cycle). Left column: experiment performed under a light intensity I ~ 25 µE m^{-2} s^{-1}; right column: I ~ 50 µE m^{-2} s^{-1}.
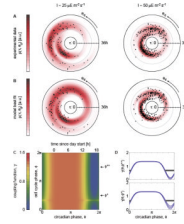
Fig. 4. Inferred coupling function

(**A**) Joint distribution of circadian phase at division and lifetime of all tracked cells. The color-coded density is a Gaussian-kernel average with a width corresponding to 2 hours along each direction. (**B**) Same data as in **A** but with density corresponding to the best fit to both data sets. For **A** and **B**, left column: I ~ 25 µE m^{-2} s^{-1}, right column: I ~ 50 µE m^{-2} s^{-1}. (**C**) Inferred coupling function obtained by averaging across parameters sampled according to their likelihood. (**D**) Confidence bands (mean ± s.d.) for the inferred coupling function across cuts parallel to the θ axis (corresponding cell cycle phases indicated with arrows in **C**). Horizontal bar: width at half maximum which quantifies gate duration. (**E**) As in **D** for cuts parallel to the ϕ axis (corresponding circadian phases indicated with dashed lines in **C**).